Broad-Band Simultaneous Measurement of the Complex Permittivity Tensor for Uniaxial Materials Using a Coaxial Discontinuity

Nour-Eddine Belhadj-Tahar and Arlette Fourrier-Lamer

Abstract—**A technique is presented for simultaneously measuring the complex values of the permittivity tensor of uniaxial materials. A gap in a coaxial line is filled with the material under test. Complex elements of the permittivity tensor are computed from measurements of the S parameters (S_{11} and S_{21}) made on the gap taking into account higher order modes excited at the discontinuity. Measured complex permittivity data are presented from 45 MHz up to 18 GHz. This technique shows good agreement between calculated and generally accepted values.**

I. Introduction

In the microwave frequency range, experimental methods for determining the constitutive parameters of anisotropic materials have been investigated by various authors [1]–[4]. The measurements may be performed by means of the perturbation of cavity resonators, inside a rectangular waveguide, or in free space. However, these methods are limited in frequency or are applicable only to particular materials [5]. The techniques using H modes or TEM modes require various locations of the sample relative to the electric field.

The solution presented here uses an inner coaxial conductor discontinuity into which the sample to be measured is easily inserted. The electromagnetic analysis of the structure (direct problem) is valid irrespective of the size of the sample and the working frequency. The uncertainty arising from an error in sample dimensions is not a main factor in this method. For this study we use "mode matching," the method used previously [6], [7] to define the different modes excited by the discontinuity. The generation of higher order waves of the transverse magnetic type allows the simultaneous determination of the elements of the permittivity tensor without any manipulation of the sample. The determination of elements of the permittivity tensor from S_{11} and S_{21} measurements (inverse problem) is linked to two infinite systems of simultaneous equations. We demonstrate that this problem is reduced to two systems, each containing three equations with three unknowns. Computer time is therefore reasonable without affecting accuracy.

Manuscript received July 21, 1990; revised April 12, 1991.

The authors are with the Laboratoire de Dispositifs Infrarouge et Microondes (ID 5450), Université Pierre et Marie Curie, Tour 12, Etage 2, 4, Place Jussieu 75252 Paris Cedex 05, France.

IEEE Log Number 9102321.

II. Direct Problem

A. Formulation of the Problem

We examine the structure shown in Fig. 1. The interruption of the inner conductor of the coaxial line constitutes a circular waveguide filled with a homogeneous and nonmagnetic material. The sample, of thickness $2d$, is assumed to be uniaxially anisotropic. The complex permittivity may be represented with the dielectric tensor:

$$[\epsilon_d] = \begin{bmatrix} \epsilon_\perp & 0 & 0 \\ 0 & \epsilon_\perp & 0 \\ 0 & 0 & \epsilon_z \end{bmatrix} \tag{1}$$

with $\epsilon_\perp = \epsilon'_\perp - j\epsilon''_\perp$ and $\epsilon_z = \epsilon'_z - j\epsilon''_z$.

The coaxial line is much longer than the transverse dimensions. It is filled with air and propagates the TEM mode only. Moreover, the conductors are assumed to be perfect.

At planes $T1$ and $T2$ (the air–material interfaces) the sample can be represented as a quadrupole characterized by its $[Y]$ and $[S]$ matrices [8]. The admittances are normalized in relation to the characteristic admittance of the coaxial line. Given that the structure is symmetrical, the representations used are also symmetrical (Fig. 1). In this case the relationships between the elements of the admittance matrix and those of the scattering matrix are easily obtained:

$$S_{11} = S_{22} = \frac{1 - y_{11}(y_{11} + 2y_{12})}{(1 + y_{11})(1 + y_{11} + 2y_{12})} \tag{2}$$

$$S_{21} = S_{12} = \frac{2y_{12}}{(1 + y_{11})(1 + y_{11} + 2y_{22})}. \tag{3}$$

Let us apply the bisection theorem to the sample and to the quadrupole. In the presence of an electric wall placed

0018-9480/91/1000-1718$01.00 ©1991 IEEE

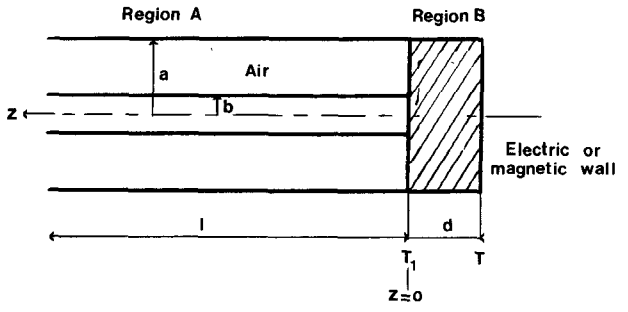

Fig. 1. Geometry of the structure and equivalent representations.

at plane T, the normalized input admittance at plant $T1$ is

$$y_e = y_{11} + 2y_{12}. \tag{4}$$

If a magnetic wall is next placed at plane T, the input admittance is

$$y_m = y_{11}. \tag{5}$$

As a result, (2) and (3) can be written as

$$S_{11} = S_{22} = \frac{1 - y_m y_e}{(1+y_m)(1+y_e)} \tag{6}$$

$$S_{21} = S_{12} = \frac{y_e - y_m}{(1+y_m)(1+y_e)}. \tag{7}$$

Equations (6) and (7) enable us to link the measurements of the S parameters to the dielectric properties of the material placed in the cell. To calculate the input impedance y_e and y_m we used the same electromagnetic analysis as used in [6] and [7].

B. Fields in the Structure

Let us consider a TEM wave propagating in region A of Fig. 2. In region B, the medium anisotropy is uniaxial. Pure E and H modes are then possible [9]. The cylindrical symmetry enables us to predict that only E modes independent of the azimuthal angle ϕ will be excited at the $z = 0$ plane. To be unhampered by the line excitation method, we take a length of coaxial line which is much longer than the transverse dimensions so that the higher order modes created by the source are not superposed on the higher order modes excited by the discontinuity.

It is well known that the E modes in a waveguide can be derived from an electrical-type Hertzian potential function, $\vec{\pi}_e = \pi_e \vec{z}$, by means of the following equations [10]:

$$\vec{H} = -\vec{\text{rot}}\ \vec{\pi}_e \tag{8}$$

$$j\omega\epsilon_0[\epsilon]\vec{E} = -\vec{\text{rot}}\ \vec{\text{rot}}\ \vec{\pi}_e \tag{9}$$

where a time dependence of $\exp(j\omega t)$ is assumed. The quantities ϵ_0 and μ_0 are, respectively, the permeability

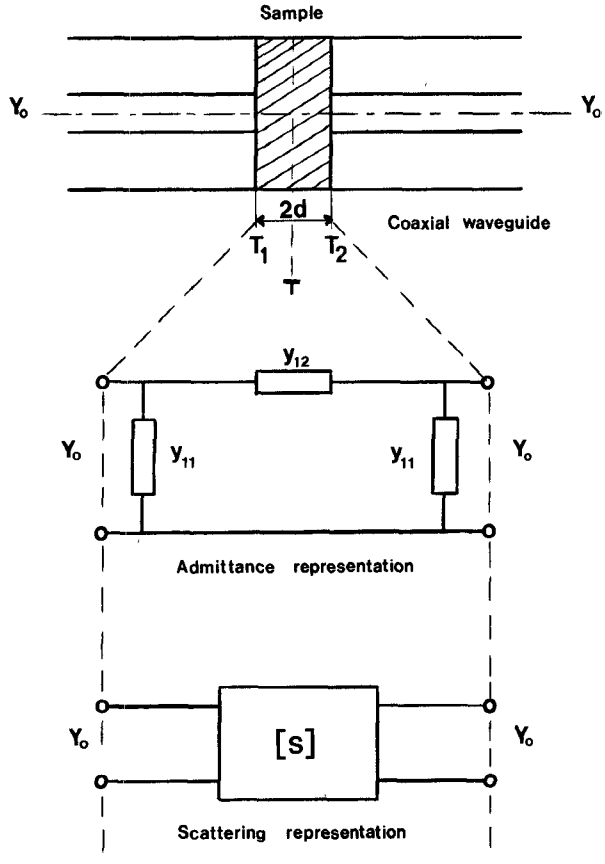

Fig. 2. Representation of the bisected structure.

and permittivity in free space; $\omega = 2\pi f$; f is the operating frequency; $\vec{z}$ is the unit vector in the z direction; and

$$[\epsilon] = 1, \qquad z > 0 \tag{10}$$

$$[\epsilon] = [\epsilon_d], \qquad z < 0. \tag{11}$$

For $z > 0$, π_e satisfies the Helmotz equation

$$(\Delta + k_0^2)\pi_e = 0 \tag{12}$$

where $k_0^2 = \omega^2 \mu_0 \epsilon_0$. However, owing to the presence of the anisotropic dielectric where $z < 0$, it can be easily shown that π_e is a solution of

$$\Delta_T \pi_e + p^2 \frac{\partial^2 \pi_e}{\partial z^2} + k_0^2 \epsilon_z \pi_e = 0 \tag{13}$$

where

$$p^2 = \frac{\epsilon_z}{\epsilon_\perp} \tag{14}$$

and

$$\Delta_T = \Delta - \frac{\partial^2}{\partial z^2}. \tag{15}$$

If a solution for π_e of the form $\psi(r,\phi)\exp \pm \gamma_z$ is assumed, the function ψ satisfies the following two-dimen-

sional scalar Helmotz equation:

$$\Delta_T \psi^{(A)}(r,0) + \zeta^2 \psi^{(A)}(r,0) = 0, \qquad z > 0 \tag{16}$$

$$\Delta_T \psi^{(B)}(r,0) + \lambda^2 \psi^{(B)}(r,0) = 0, \qquad z < 0. \tag{17}$$

In circular cylindrical coordinates, the solution for the E modes independent of azimuthal angle ϕ is

$$\psi_q^{(A)} = C_q Z_0(\zeta_q r) \qquad z > 0 \tag{18}$$

$$\psi_i^{(B)} = D_i J_0(\lambda_i r) \qquad z < 0 \tag{19}$$

where

$$\zeta_q^2 = k_0^2 + \gamma_q^2, \qquad q = 1,2,\cdots \tag{20}$$

$$\lambda_i^2 = \epsilon_z k_0^2 + p^2 \gamma_i^2, \qquad i = 1,2,\cdots. \tag{21}$$

C_q and D_i are constants and Z_0 is the linear combination of Bessel functions of the first and second kinds as follows:

$$Z_0(\zeta_q r) = J_0(\zeta_q r) + G_{Aq} N_0(\zeta_q r) \tag{22}$$

where G_{Aq} is a constant.

Once $\psi_q^{(A)}$ and $\psi_i^{(B)}$ are known, the components of the E modes in each region, A and B, are found easily.

In the air-filled region A, the components of the total electromagnetic field are

$$E_{rA} = \frac{1}{r} A_0 [\exp(+jk_0 z) + \Gamma \exp(-jk_0 z)] + \sum_{q=1}^{\infty} A_q Z_1(\zeta_q r) \exp(-\gamma_q z) \tag{23}$$

$$E_{zA} = \sum_{q=1}^{\infty} A_q \frac{\zeta_a}{\gamma_q} Z_0(\zeta_q r) \exp(-\gamma_q z) \tag{24}$$

$$H_{\phi A} = \frac{1}{r} A_0 Y_{A0} [\exp(+jk_0 z) - \Gamma \exp(-jk_0 z)] + \sum_{q=1}^{\infty} A_q Y_{Aq} Z_1(\zeta_q r) \exp(-\gamma_q z) \tag{25}$$

where

$$A_q = -\frac{\zeta_a \gamma_q}{j\omega\epsilon_0} C_q. \tag{26}$$

A_0 represents the incident TEM wave amplitude and Γ its reflection coefficient at plane $T1$ of the discontinuity; Y_{A0} and Y_{Aq} are, respectively, the wave admittances of the TEM mode and the higher order mode E_{0q} in the coaxial waveguide:

$$Y_{A0} = -\sqrt{\frac{\epsilon_0}{\mu_0}} \tag{27}$$

$$Y_{Aq} = \frac{j\omega\epsilon_0}{\gamma_q} \tag{28}$$

and

$$\gamma_q^2 = \zeta_q^2 - k_0^2. \tag{29}$$

In (23), (24), and (25) Z_p denotes the linear combination of the pth-order Bessel functions of the first and second kinds as follows:

$$Z_p(\zeta_q r) = J_p(\zeta_q r) + G_{Aq} N_p(\zeta_q r) \tag{30}$$

with $p = 0$ or 1.

When an electric wall is placed at plane T, the electric field boundary conditions at this plane provide the solutions for region B:

$$E_{rB} = \sum_{i=1}^{\infty} B_i' J_1(\lambda_i r) \sinh \gamma_i (z + d) \tag{31}$$

$$E_{zB} = \sum_{i=1}^{\infty} -\frac{\epsilon_\perp}{\epsilon_z} \cdot \frac{\lambda_i}{\gamma_i} B_i' J_0(\lambda_i r) \cosh \gamma_i (z + d) \tag{32}$$

$$H_{\phi B} = \sum_{i=1}^{\infty} -j \frac{\omega \epsilon_0 \epsilon_\perp}{\gamma_i} B_i' J_1(\lambda_i r) \cosh \gamma_i (z + d) \tag{33}$$

with

$$B_i' = 2 D_i \frac{\lambda_i \gamma_i}{j\omega\epsilon_0\epsilon_\perp} \exp(-\gamma_i d) \tag{34}$$

and

$$\gamma_i^2 = \frac{\epsilon_\perp}{\epsilon_z} \lambda_i^2 - \epsilon_\perp k_0^2. \tag{35}$$

The axial component E_z for the electric field for each E wave must be zero at the conductors in the two regions. The following conditions are thus obtained:

$$Z_0(\zeta_q a) = Z_0(\zeta_q b) = 0 \tag{36}$$

$$J_0(\lambda_i a) = 0. \tag{37}$$

Relation (36) enables us to determine the coefficient G_{Aq} contained in (22) and (30):

$$G_{Aq} = -\frac{J_0(\zeta_q a)}{N_0(\zeta_q a)} = -\frac{J_0(\zeta_q b)}{N_0(\zeta_q b)} \tag{38}$$

and, thus, from the following transcendental equation, the coefficient ζ_q:

$$J_0(\zeta_q a) N_0(\zeta_q b) - J_0(\zeta_q b) N_0(\zeta_q a) = 0. \tag{39}$$

The boundary conditions for the transverse components at the plane T_1 are expressed in the following manner:

$$E_{rB} = 0, \qquad 0 < r < b \tag{40}$$

$$E_{rB} = \sum_{i=1}^{\infty} B_i J_1(\lambda_i r) = \frac{1}{r} A_0 (1 + \Gamma) + \sum_{q=1}^{\infty} A_q Z_1(\zeta_{qr}), \qquad b < r < a \tag{41}$$

$$H_{\phi B} = \sum_{i=1}^{\infty} B_i Y_{ei} J_1(\lambda_i r) = \frac{1}{r} A_0 Y_{A0} (1 - \Gamma) + \sum_{q=1}^{\infty} A_q Y_{Aq} Z_1(\zeta_q r), \qquad b < r < a \tag{42}$$

where

$$B_i = B_i' \sinh \gamma_i d \tag{43}$$

and

$$Y_{ei} = -j\frac{\omega\epsilon_0\epsilon_\perp}{\left(\frac{\epsilon_\perp}{\epsilon_z}\lambda_i^2 - \epsilon_\perp k_0^2\right)^{1/2}} \coth\left[\left(\frac{\epsilon_\perp}{\epsilon_z}\lambda_i^2 - \epsilon_\perp k_0^2\right)^{1/2} d\right]. \tag{44}$$

Coefficients A_q and B_i are determined by using the orthogonality properties of Bessel functions. The first step is to perform the following integral:

$$\int_0^a rJ_1(\lambda_j r)E_{rB}\,dr. \tag{45}$$

Using Lommel integrals and equalities (40), (41), (36), and (37), we obtain

$$\frac{B_i}{\lambda_i} = A_0(1+\Gamma)\frac{2J_0(\lambda_i b)}{\lambda_i^2 a^2 J_1^2(\lambda_i a)} \cdot\left(1 - \sum_{q=1} \frac{A_q}{A_0(1+\Gamma)} \cdot \frac{bZ_1(\zeta_q b)}{\zeta_q^2/\lambda_i^2 - 1}\right). \tag{46}$$

Next, $H_{\phi B}$ is integrated over the range $b < r < a$. Relations (42), (36), and (37) give

$$A_0 Y_{A0}(1-\Gamma)\ln\frac{a}{b} = \sum_{i=1}^{\infty} \frac{B_i Y_{ei}}{\lambda_i^0} J_0(\lambda_i b). \tag{47}$$

The last step is to integrate the quantity $rZ_1(\zeta_n r)H_{\phi B}$ over the range $b < r < a$. Hence

$$\frac{Y_{An}}{2} A_n b Z_1(\zeta_n b)\left[\frac{a^2 Z_1^2(\zeta_n a)}{b^2 Z_1^2(\zeta_n b)} - 1\right] = \sum_{i=1}^{\infty} \frac{B_i Y_{ei}\lambda_i J_0(\lambda_i b)}{\lambda_i^2 - \zeta_n^2}. \tag{48}$$

The normalized input admittance y in plane T_1 may be written in the following form: $1-\Gamma/1+\Gamma$. Equations (46) and (47) allow us derive the solution:

$$y_e = j\frac{2k_0 a\epsilon_\perp}{\ln\frac{a}{b}} \cdot \sum_{i=1}^{\infty} \frac{J_0^2(\lambda_i b)\coth\left[\left(\frac{\epsilon_\perp}{\epsilon_z}\lambda_i^2 a^2 - \epsilon_\perp k_0^2 a^2\right)^{1/2} d/a\right]}{\left(\frac{\epsilon_\perp}{\epsilon_z}\lambda_i^2 a^2 - \epsilon_\perp k_0^2 a^2\right)^{1/2} \lambda_i^2 a^2 J_1^2(\lambda_i a)} \cdot\left(1 - \sum_{q=1}^{\infty} \frac{A_q}{A_0(1+\Gamma)} \cdot \frac{bZ_1(\zeta_q b)}{\zeta_q^2/\lambda_i^2 - 1}\right) \tag{49}$$

or, alternatively,

$$y_e = j\frac{2k_0 a\epsilon_\perp}{\ln\frac{a}{b}}\left(y_0 - \sum_{q=1}^{\infty} y_q x_q\right) \tag{50}$$

where

$$y_0 = \sum_{i=1}^{\infty} \frac{\coth\left[\left(\frac{\epsilon_\perp}{\epsilon_z}\lambda_i^2 a^2 - \epsilon_\perp k_0^2 a^2\right)^{1/2} d/a\right]}{\left(\frac{\epsilon_\perp}{\epsilon_z}\lambda_i^2 a^2 - \epsilon_\perp k_0^2 a^2\right)^{1/2} \lambda_i^2 a^2} \cdot \frac{J_0^2(\lambda_i b)}{J_1^2(\lambda_i a)} \tag{51}$$

$$x_q = \frac{A_q}{A_0(1+\Gamma)} bZ_1(\zeta_q b) \tag{52}$$

$$y_q = -\sum_{i=1}^{\infty} \frac{\coth\left[\left(\frac{\epsilon_\perp}{\epsilon_z}\lambda_i^2 a^2 - \epsilon_\perp k_0^2 a^2\right)^{1/2} d/a\right]}{\left(\frac{\epsilon_\perp}{\epsilon_z}\lambda_i^2 a^2 - \epsilon_\perp k_0^2 a^2\right)^{1/2} \left(\lambda_i^2 a^2 - \zeta_q^2 a^2\right)} \cdot \frac{J_0^2(\lambda_i b)}{J_1^2(\lambda_i a)}. \tag{53}$$

The coefficients x_q are obtained from (48) using relations (46), (44), and (28). This leads to the matrix equation

$$\begin{aligned}\frac{1}{\epsilon_\perp} \cdot \frac{x_n}{4\left(\zeta_n^2 a^2 - k_0^2 a^2\right)^{1/2}}&\left[\frac{a_1^2 Z_1^2(\zeta_n a)}{b_1^2 Z_1^2(\zeta_n b)} - 1\right] \\ &= \sum_{i=1}^{\infty} - \frac{\coth\left[\left(\frac{\epsilon_\perp}{\epsilon_z}\lambda_i^2 a^2 - \epsilon_\perp k_0^2 a^2\right)^{1/2} d/a\right]}{\left(\frac{\epsilon_\perp}{\epsilon_z}\lambda_i^2 a^2 - \epsilon_\perp k_0^2 a^2\right)^{1/2} \left(\lambda_i^2 a^2 - \zeta_n^2 a^2\right)} \cdot \frac{J_0^2(\lambda_i b)}{J_1^2(\lambda_i a)} \\ &\quad - \sum_{i=1}^{\infty}\sum_{q=1}^{\infty} x_q \frac{\lambda_i^2 a^2 \coth\left[\left(\frac{\epsilon_\perp}{\epsilon_z}\lambda_i^2 a^2 - \epsilon_\perp k_0^2 a^2\right)^{1/2} d/a\right]}{\left(\frac{\epsilon_\perp}{\epsilon_z}\lambda_i^2 a^2 - \epsilon_\perp k_0^2 a^2\right)^{1/2} \left(\lambda_i^2 a^2 - \zeta_q^2 a^2\right)\left(\lambda_i^2 a^2 - \zeta_n^2 a^2\right)} \cdot \frac{J_0^2(\lambda_i b)}{J_1^2(\lambda_i a)}\end{aligned} \tag{54}$$

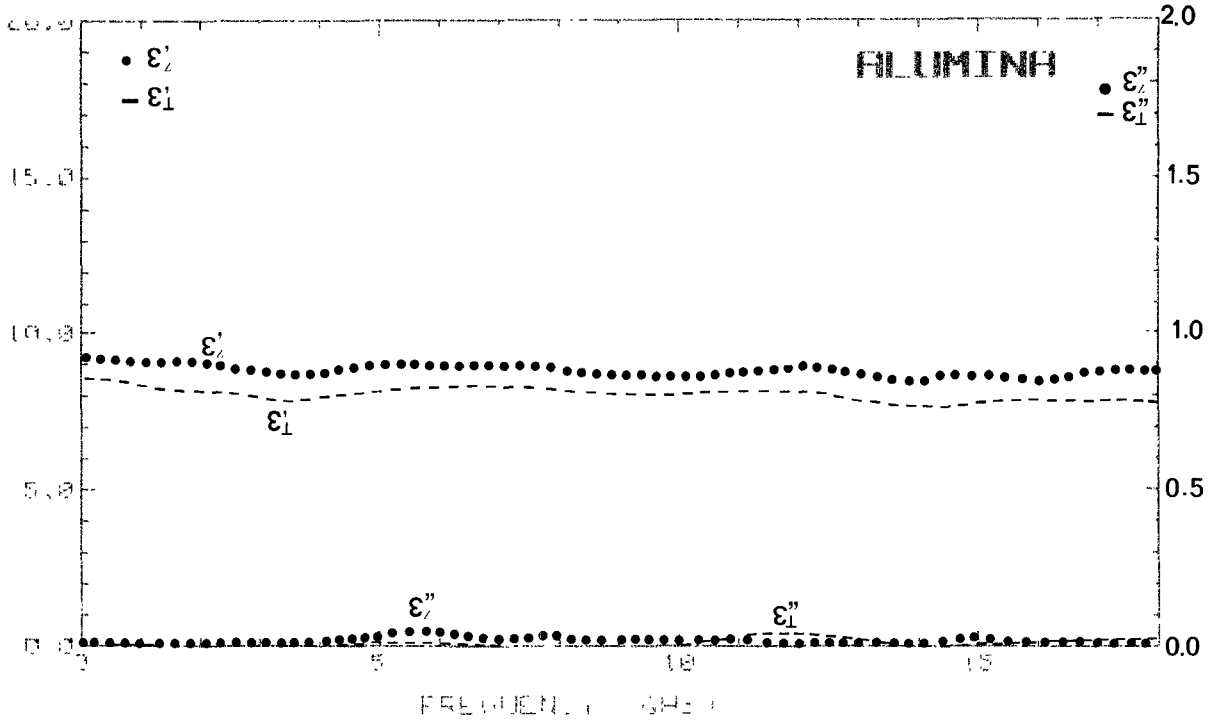

Fig. 3. Complex permittivity tensor measured for an alumina sample in the 45 MHz–18 GHz frequency range; thickness = 2 mm; APC7-mm standard.

or, alternatively,

$$\sum_{q=1}^{\infty} A_{qn} x_q = y_n, \qquad n = 1,2,\cdots \tag{55}$$

where

$$A_{qn} = \sum_{i=1}^{\infty} \frac{\lambda_i^2 a^2 \coth\left[\left(\frac{\epsilon_\perp}{\epsilon_z}\lambda_i^2 a^2 - \epsilon_\perp k_0^2 a^2\right)^{1/2} d/a\right]}{\left(\frac{\epsilon_\perp}{\epsilon_z}\lambda_i^2 a^2 - \epsilon_\perp k_0^2 a^2\right)^{1/2}\left(\lambda_i^2 a^2 - \zeta_q^2 a^2\right)\left(\lambda_i^2 a^2 - \zeta_n^2 a^2\right)} \cdot \frac{J_0^2(\lambda_i b)}{J_1^2(\lambda_i a)} + \frac{1}{\epsilon_\perp} \frac{\delta_{qn}}{4\left(\zeta_n^2 a^2 - k_0^2 a^2\right)^{1/2}}\left[\frac{a_i^2 Z_1^2(\zeta_n a)}{b_1^2 Z_1^2(\zeta_n b)} - 1\right] \tag{56}$$

with δ_{qn} the Kronecker delta function.

If a magnetic wall is placed in the bisection plane T, the transverse components of the total electromagnetic field in region B are

$$E_{rB} = \sum_{i=1}^{\infty} B_i'' J_1(\lambda_i r)\cosh\gamma_i(z+d) \tag{57}$$

$$H_{\phi B} = \sum_{i=1}^{\infty} -j\frac{\omega\epsilon_0\epsilon_\perp}{\gamma_i} B_i'' J_1(\lambda_i r)\sinh\gamma_i(z+d). \tag{58}$$

At the reference plane T_1 these components can be written as follows:

$$E_{rB} = \sum_{i=1}^{\infty} B_i J_1(\lambda_i r) \tag{59}$$

$$H_{\phi B} = \sum_{i=1}^{\infty} B_i Y_{mi} J_1(\lambda_i r) \tag{60}$$

with

$$B_i = B_i'' \cosh\gamma_i d \tag{61}$$

and

$$Y_{mi} = -j\frac{\omega\epsilon_0\epsilon_\perp}{\left(\frac{\epsilon_\perp}{\epsilon_z}\lambda_i^2 - \epsilon_\perp k_0^2\right)^{1/2}} \tanh\left[\left(\frac{\epsilon_\perp}{\epsilon_z}\lambda_i^2 - \epsilon_\perp k_0^2\right)^{1/2} d\right]. \tag{62}$$

Hence, the same procedure is adopted to calculate the input admittance y_m. We find the same results in replacing coth( ) with tanh( ) in (40) to (56):

$$y_m = j\frac{2k_0 - a\epsilon_\perp}{\ln\frac{a}{b}}\left(y_0' - \sum_{q=1}^{\infty} y_q' x_q'\right). \tag{63}$$

C. Numerical Computation

The S-parameter computation starts with the evaluation of quantities λ_i and ζ_q from a Bessel subroutine. The roots of transcendental equations (37) and (39) are found by iteration. Bessel functions are programmed in the

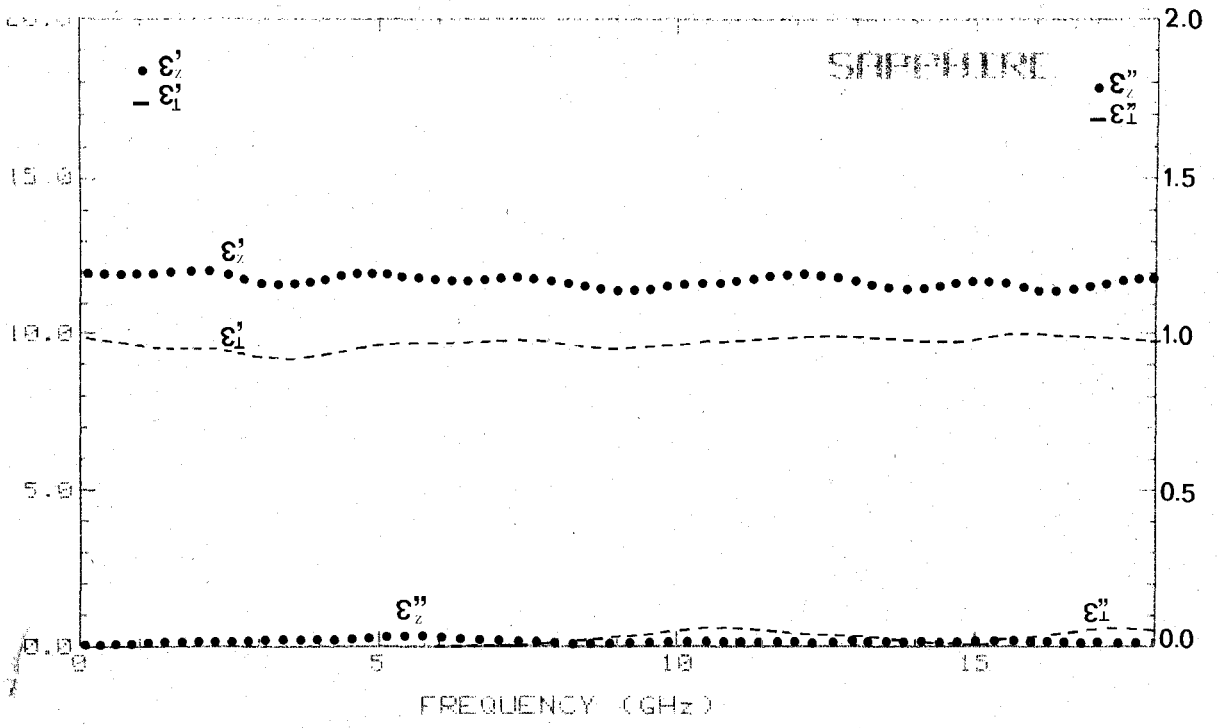

Fig. 4. Complex permeability tensor measured for a sapphire sample in the 45 MHz–18 GHz frequency range; thickness = 2 mm; APC7-mm standard.

polynomial approximation form [11]. Hence, for a given frequency and for a material of known properties, coefficients y_0 and y_q can be computed in both cases of electric and magnetic walls if the summation over i is truncated. In fact, this truncation is used to retain a finite number of higher order modes excited by the discontinuity and present in the sample ($i = 1, 2, \cdots, I$). In the same manner, to compute the coefficient A_{qn}, we retain a number Q of higher order modes excited in the coaxial waveguide by the discontinuity. Hence (55) is reduced to two systems of Q equations with Q unknowns x_q ($q = 1, 2, \cdots, Q$). From this, y_e and y_m values are obtained. The effect on the admittance computation accuracy of the number of higher order modes retained has been described in [7] and [12] and by other authors [13], [14]. We show that the accuracy is better than 0.1% if we take $I = 2Q = 6$ [12].

III. Inverse Problem

This section involves the complex permittivity tensor computation from S-parameter measurements of the gap filled by the uniaxial sample. To avoid contact resistances and contact capacitances, the sample is metallized on the contact surfaces with the line conductors. The simultaneous calculation of $\epsilon_\perp = \epsilon'_\perp - j\epsilon''_\perp$ and $\epsilon_z = \epsilon'_z - j\epsilon''_z$ is carried out by comparison between measured and calculated S_{11} and S_{21} values. For this purpose we use the same iterative method as used before [7]. This method is derived from the gradient method. The number of iterations is fixed by the instrumentation error of the network analyzer.

IV. Experimental Results

The results of the measurements on sapphire and alumina (99.7%) are represented in Figs. 3 and 4. The measurements performed on each of these materials were obtained at room temperature using the HP8510B network analyzer in an APC7 standard line. The thickness of each sample was 2 mm. Anisotropy is a well-known property of sapphire, i.e., a single crystal of aluminum oxide. In polycrystalline alumina, a preferred orientation of the crystallites can sometimes be observed [15], [16]. In sapphire, the value of ϵ'_z in the direction of the optic axis is 11.5 according to [17] or 11.7 according to [15]. Perpendicular to the optic axis, $\epsilon'_\perp = 9.5$ [17] or 9.34 [16]. For alumina without a preferred orientation, $\epsilon'_\perp = \epsilon'_z = 8.76$ is given in [16] and 9.7 in [15]. These two materials show very low losses (ϵ'' being lower than 0.001). The values measured, depicted in Figs. 3 and 4, correspond to those anticipated. However, because of the large errors in small $\epsilon''_\perp$ and ϵ''_z, the measurement of ϵ'' for low-loss samples is difficult with this technique. The accuracy of the method was computed by simulation on a calculator. The calculator, programmed for the HP8510B system instrumentation errors, together with the measurements of the S_{11} and S_{21} values, allows the measuring errors in $\epsilon_\perp$ and ϵ_z to be determined. To obtain good ϵ'' accuracy, $\epsilon''_\perp$ and ϵ''_z should be greater than 0.1. The accuracy is better than 4% for ϵ' and for the higher values of ϵ'' ($\epsilon'' > 1$). For the low losses, the ϵ'' accuracy is better than 10%. The uncertainty for $\epsilon_\perp$ and ϵ_z caused by a small error in the physical length of the sample is practically equal to the percentage of the error. Since it is easy to measure

the sample length to an accuracy within ± 0.01 mm, the uncertainty caused by an error in the length of the sample material is not a significant factor in this measurement method.

V. Conclusion

A broad-band technique is presented for simultaneously measuring the complex elements of the permittivity tensor of homogeneous uniaxial materials. The material under test fills a gap in a coaxial line. To avoid contact resistances and contact capacitances, the sample is metallized on the contact surfaces with the line conductors. Required dimensional tolerances are 0.01 mm. Values for $\epsilon_\perp$ and ϵ_z are computed from S_{11} and S_{21} measurements made on an automated network analyzer. This method is easy to use and requires no corrections in experimental results. With a single sample, it allows continuous characterization up to 18 GHz. By using APC2.4 connections, the method can be extended up to 50 GHz.

References

[1] W. V. Aulock and J. H. Rowen, "Measurement of dielectric and magnetic properties of ferromagnetic materials at microwave frequencies," *Bell Syst. Tech. J.*, vol. 36, no. 2, pp. 427–448, 1957.

[2] H. E. Bussey and L. A. Steinert, "An exact solution for cylindrical cavity containing a gyromagnetic material," *Proc. IRE*, p. 693, May 1957.

[3] N. J. Damaskos, R. B. Mack, A. L. Maffett, W. Parmon, and P. L. E. Uslenghi, "The inverse problem for biaxial materials," *IEEE Trans. Microwave Theory Tech.*, vol. MTT-32, pp. 400–405, Apr. 1984.

[4] O. Hashimoto and Y. Shimuzi, "Reflecting characteristics of anisotropic rubber sheets and measurements of complex permittivity tensor," *IEEE Trans. Microwave Theory Tech.*, vol. MTT-34, pp. 1202–1207, Nov. 1986.

[5] J. P. Parneix, C. Legrand, and S. Toutain, "Automatic permittivity measurements in a wide frequency range: application to anisotropic fluid," *IEEE Trans. Microwave Theory Tech.*, vol. MTT-30, pp. 2015–2017, Nov. 1982.

[6] N. E. Belhadj-Tahar and A. Fourrier-Lamer, "Broad-band analysis of a coaxial discontinuity used for dielectric measurements," *IEEE Trans. Microwave Theory Tech.*, vol. MTT-34, pp. 346–350, Mar. 1986.

[7] N. E. Belhadj-Tahar, A. Fourrier-Lamer, and H. de Chanterac, "Broad-band simultaneous measurement of complex permittivity and permeability using a coaxial discontinuity," *IEEE Trans. Microwave Theory Tech.*, vol. 38, pp. 1–7, Jan. 1990.

[8] M. Sucher and J. Fox, *Handbook of Microwave Measurements*, 3rd ed. New York: Wiley, 1963, vol. II.

[9] J. A. Kong and D. K. Cheng, "On guided waves in moving anisotropic media," *IEEE Trans. Microwave Theory Tech.*, vol. MTT-16, pp. 99–103, Feb. 1968.

[10] C. T. M. Chang, "Circular waveguides lined with artificial anisotropic dielectrics," *IEEE Trans. Microwave Theory Tech.*, vol. MTT-20, pp. 517–523, Aug. 1972.

[11] M. Abramowitz and I. A. Stegun, *Handbook of Mathematical Functions*. Washington, DC: Government Printing Office, National Bureau of Standards, ch. 9, sect. 4, pp. 369–370.

[12] N. E. Belhadj-Tahar and A. Fourrier-Lamer, "Utilisation pratique d'une cellule très large bande pour la mesure automatique de la permittivité de divers matériaux," *L'Onde Electrique*, vol. 68, pp. 50–59, Jan. 1988.

[13] P. H. Masterman and P. J. B. Clarricoats, "Computer field-matching solution of waveguide transverse discontinuities," *Proc. Inst. Elec. Eng.*, vol. 118, pp. 51–63, Jan. 1971.

[14] W. J. English, "The circular waveguide step-discontinuity mode transducer," *IEEE Trans. Microwave Theory Tech.*, vol. MTT-21, pp. 633–636, Oct. 1973.

[15] J. H. C. van Heuven and T. H. A. M. Vlek, "Anisotropy in alumina substrates for microstrip circuits," *IEEE Trans. Microwave Theory Tech.*, vol. MTT-20, pp. 775–777, Nov. 1972.

[16] J. E. Aitken, P. H. Ladbrooke, and M. H. N. Potok, "Microwave measurement of the temperature coefficient of permittivity for sapphire and alumina," *IEEE Trans. Microwave Theory Tech.*, vol. MTT-23, pp. 526–529, June, 1975.

[17] W. H. Gitzen, "Alumina as a ceramic material," *U.S.A.: American Ceramic Society*, p. 78, 1970.

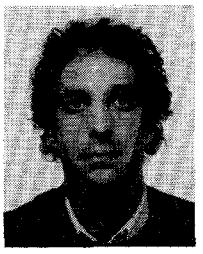

Nour-Eddine Belhadj-Tahar received the Dipl.-Ing. degree in electrical engineering from the University of Sciences and Technology of Oran, Algeria, in 1977, and the Ph.D. degree (Doctorat de l'Université Pierre et Marie Curie) in electrical engineering from the University Pierre et Marie Curie—PARIS VI in 1986.

From 1980 to 1982, he was with the Institute of Physics, University of Tlemcen, Algeria, where he held the position of Assistant Professor. In 1983, he joined the University Pierre et Marie Curie—PARIS VI, where he is presently Assistant Professor. His research has dealt with electromagnetic wave propagation and microwave and millimeter-wave dielectric measurements techniques.

Arlette Fourrier-Lamer received the Ph.D. degree (Doctorat d'Etat es Sciences Physiques) in 1981.

She is Professor of Electronic Engineering at the University of PARIS VI—Pierre et Marie Curie. Her research has dealt with electronic and nuclear double resonance (ENDOR) in paramagnetic liquids. Since 1982, she has also been working on electromagnetic discontinuities and applications to materials characterization (resins, conducting polymers, superconductors, ferrites).

Dr. Fourrier-Lamer is a member of the Société Française des Electroniciens et des Radioélectriciens (SEE).